



SHEARLET-BASED INVERSE HALFTONING

¹CHENGZHI DENG, ¹WEI TIAN, ²SAIFENG HU, ¹YAN LI

¹Department of Information Engineering, Nanchang Institute of Technology, Nanchang, China

² Education Evaluation Center, Nanchang Institute of Technology, Nanchang, China

E-mail: dengchengzhi@126.com

ABSTRACT

Under the linear approximation model for error diffusion halftoning, a shearlet-based inverse halftoning (SIH) algorithm is proposed. The SIH algorithm performs inverse halftoning by first inverting the model-specified convolution operator and then reducing the residual color noise using scalar shearlet-domain thresholding. The optimal thresholds are derived by using the maximum a posteriori rule. Experimental results demonstrate that SIH algorithm is competitive with state-of-the-art classical inverse techniques in peak signal-to-noise ratio (PSNR) sense. And the SIH algorithm also provides good visual quality.

Keywords: *Error diffusion, inverse halftoning, shearlet transform, maximum a posteriori rule*

1. INTRODUCTION

The process of rendition from continuous-tone images into a medium on which only two levels can be displayed is defined as digital halftoning. The rendered bi-level image is referred to as halftone. Inverse halftoning is the process of retrieving the continuous-tone image from its halftoned version. The inverse halftoning algorithms can be classified into two categories, the filtering-based algorithm and the learning-based algorithm. The typical filtering-based algorithms include wavelet-based approaches [1], Bayesian methods [2], and human visual system-based approaches [3]. The learning-based algorithm mainly include vector quantization methods [4], lookup table-based algorithms [5] and neural network-based algorithms [6]. The inverse halftoning has been used in rehalftoning, halftone resizing, halftone tone correction, and facsimile image compression.

Error-diffused halftoning is a nonlinear system because it uses a quantizer to generate halftones. Recently, Kite [7] proposed an accurate linear approximation model for error diffusion halftoning. Under this model, inverse halftoning can be posed as the classical deconvolution problem. The gray-scale image can be obtained from the halftone by deconvoluting the filter in the presence of the colored noise. Traditionally, the deconvolution is performed in the Fourier domain. Unfortunately, the Fourier-based deconvolution techniques induce ringing and blurring artifacts due to the non-sparsity representation of Fourier transform for edge discontinuities.

In contrast, the wavelet transform provides an economical representation for images with edges. The economy has led to powerful image estimation algorithms based on scalar wavelet shrinkage. In [1, 8], the wavelet was first exploited in inverse halftoning. In [9], the redundant wavelet was used to improve error-diffused halftones. However, when wavelet is used to image inverse halftoning, it will lead to oscillatory artifacts along the edges. That is why wavelet fails to capture the geometric regularity along the singularities of surfaces.

In order to overcome this limitation of traditional wavelet, several image representations have been proposed to capture the geometric regularity of a given image. They include curvelet, contourlet and bandelet. Within recent years, Demerit and his collaborator developed a new geometric multiscale transform, named shearlet transform [10-12]. The shearlet transform breaks the limitation of the wavelet transform and provides sparse representation for the objects with singularities. Now the applications of shearlet are mainly in image restoration [13], edge detection [14] and image fusion [15]. Its applications in image inverse halftoning are still under exploring.

In this paper, we propose a shearlet-based inverse halftoning (SIH) algorithm. The SIH algorithm performs inverse halftoning by first inverting the model-specified convolution operator and then reducing the residual color noise using scalar shearlet-domain thresholding. The paper is organized as follows. In section 2 we will introduce the shearlet transform. Section 3 introduces the



proposed Inverse half-toning algorithm. Experiments and results will be given in section 4. And conclusions are drawn in section 5.

2. SHEARLET TRANSFORM

The shearlet transform is a multiresolution representation with basis functions well localized in space, frequency and orientation. It is generated by one single function which is dilated by a parabolic scaling and a shear matrix and translated in the time domain. The shearlet mother function is a composite wavelet that satisfies appropriate admissibility conditions [10].

The composite wavelet, recently introduced in [11], exhibits the geometric and multiscale properties by taking advantage of classical theory of affine systems. In dimension $n = 2$, the affine systems with composite dilations are defined as follows.

$$Y_{AB}(\gamma) = \{y_{j,k,l}(\mathbf{x}) = |\det A|^{j/2} \gamma(B^j A^j \mathbf{x} - k)\} \quad (1)$$

where $Y \in L^2(\mathbb{R}^2)$, A, B are both 2×2 invertible matrices, $|\det B| = 1$. The elements of this system are called wavelet if $Y_{AB}(\gamma)$ forms a Parseval frame for $L^2(\mathbb{R}^2)$.

The dilations matrices A^j and B^l are associated with scale transformations and area-preserving geometric transformations respectively. The above framework can be used to construct Parseval frames whose elements, in addition to ranging at various scale and location, also range at various orientations.

The shearlet is a special Parseval frame of composite wavelets in $L^2(\mathbb{R}^2)$. These are collections of the form $Y_{AB}(\gamma)$ where $A = A_0$ is the anisotropic dilation matrix and $B = B_0$ is the shear matrix, which are given by $A_0 = \begin{pmatrix} 2 & 0 \\ 0 & 1 \end{pmatrix}$, $B_0 = \begin{pmatrix} 1 & 1 \\ 0 & 1 \end{pmatrix}$ As described in [12], the shearlets provide a nonuniform angular covering of the frequency plane when restricted to the finite discrete setting for implementation. Thus, it is preferred to reformulate the shearlet transform with restrictions supported in the regions given by:

$$D_0 = \{(x_1, x_2) \in \mathbb{R}^2 : |x_1| \leq 1/8, |x_2/x_1| \leq 1\}$$

$$D_1 = \{(x_1, x_2) \in \mathbb{R}^2 : |x_2| \leq 1/8, |x_1/x_2| \leq 1\}$$

For any $x = (x_1, x_2) \in \mathbb{R}^2, x_1 \neq 0$, define $y^{(0)}$ as

$$\hat{y}^{(0)}(x) = \hat{y}^{(0)}(x_1, x_2) = \hat{y}_1(x_1) \hat{y}_2(x_2/x_1) \quad (2)$$

where $\hat{y}_1, \hat{y}_2 \in C^\infty(\mathbb{R})$, $\text{supp } \hat{y}_1 \subseteq [-1/2, -1/6] \cup [1/6, 1/2]$, and $\text{supp } \hat{y}_2 \subseteq [-1, 1]$. This implies that $\hat{y}^{(0)}$ is C^∞ and compactly supported with $\text{supp } \hat{y}^{(0)} \subseteq [-1/2, 1/2]^2$. In addition, assume

$$\int_{\mathbb{R}} |\hat{y}_1(2^{-j} w)|^2 = 1 \quad \text{for } |w| \leq 1/8 \quad (3)$$

And for each $j \geq 0$,

$$\int_{\mathbb{R}} |\hat{y}_2(2^j w + 1)|^2 = 1 \quad \text{for } |w| \leq 1 \quad (4)$$

The equation (3) and (4) imply that

$$\int_{\mathbb{R}^2} |\hat{y}^{(0)}(xA_0^{-j} B_0^{-l})|^2 + \int_{\mathbb{R}^2} |\hat{y}^{(0)}(2^{-j} x_1)|^2 |\hat{y}_2(2^j x_2/x_1 + 1)|^2 = 1 \quad (5)$$

for $(x_1, x_2) \in D_0$. That is, the function $\{\hat{y}^{(0)}(xA_0^{-j} B_0^{-l})\}$ forms a tiling of D_0 , and the collection $\{y_{j,k,l}^{(0)}(x) = 2^{3j/2} \gamma^{(0)}(B_0^l A_0^j x - k) : j \geq 0, -2^j \leq l \leq 2^j, k \in \mathbb{Z}^2\}$ is a Parseval frame for $L^2(D_0)$. Similarly we can construct a Parseval frame for $L^2(D_1)$. Let

$$A_0 = \begin{pmatrix} 2 & 0 \\ 0 & 1 \end{pmatrix}, B_0 = \begin{pmatrix} 1 & 1 \\ 0 & 1 \end{pmatrix} \text{ and } \gamma^1 \text{ be given by } \hat{y}^{(1)}(x) = \hat{y}^{(1)}(x_1, x_2) = \hat{y}_1(x_2) \hat{y}_2(x_1/x_2) \quad (6)$$

Then the collection $\{y_{j,k,l}^{(1)}(x) = 2^{3j/2} \gamma^{(1)}(B_1^l A_1^j x - k) : j \geq 0, -2^j \leq l \leq 2^j - 1, k \in \mathbb{Z}^2\}$ is a Parseval frame for $L^2(D_1)$. Let $j \in \mathbb{Z}$ satisfy

$$|\hat{f}(x)|^2 + \int_{\mathbb{R}^2} |\hat{y}^{(0)}(xA_0^{-j} B_0^{-l})|^2 + \int_{\mathbb{R}^2} |\hat{y}^{(1)}(xA_1^{-j} B_1^{-l})|^2 = 1$$

for $x \in \mathbb{R}^2$. Thus, we have the following:

Theorem 1: Let $j_k(x) = j(x-k)$ and $y_{j,k,l}^{(d)}(x) = 2^{3j/2} y^{(d)}(B_d^l A_d^j x - k)$, where j, y are given as above. Then the collection of shearlet: $\{j_k : k \in \mathbb{Z}^2\} \cup \{y_{j,k,l}^{(d)} : j \in \mathbb{Z}^+, l \in \mathbb{Z}^+, k \in \mathbb{Z}^2, d = 0, 1\}$ is a Parseval frame for $L^2(\mathbb{R}^2)$.

For each $f \in L^2(\mathbb{R}^2)$, the shearlet transform is the mapping on $L^2(\mathbb{R}^2)$ defined by

$$SH : f \mapsto SH_y f(j, k, l) = \langle f, y_{j,k,l}^{(d)} \rangle, d = 0, 1 \quad (7)$$

3. INVERSE HALFTONING ALGORITHM

The linear approximation model [8] for error diffusion halftoning can be expressed as follows.

$$y(i, j) = Rx(i, j) + Qg(i, j) \quad (8)$$

Where $y(i, j)$ is halftone, $x(i, j)$ and $g(i, j)$ are original image and additive white noise, respectively. The linear model is shown in figure 1.

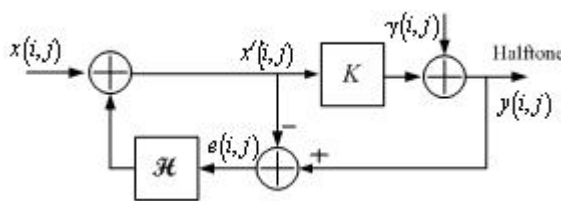


Figure 1. The linear approximation of error diffusion halftoning.

This model approximates the effects of quantization using a gain K followed by the addition of white noise. For any given error diffusion technique, Kite found that the gain K is almost constant for different images. The R and Q are the linear time-invariant system with respective impulse response $p(i, j)$ and $q(i, j)$ determined by the error diffusion technique.

$$R(w_1, w_2) = \frac{K}{1 + (K-1)H(w_1, w_2)} \quad (9)$$

$$Q(w_1, w_2) = \frac{1 - H(w_1, w_2)}{1 + (K-1)H(w_1, w_2)} \quad (10)$$

From equation (8), it can be seen that the deconvolution can be used to inverse halftoning. A

naïve deconvolution estimate $\hat{x}(i, j)$ is obtained using operator inverse R^{-1} as

$$\hat{x}(i, j) = R^{-1}y(i, j) = x(i, j) + R^{-1}Qg(i, j) \quad (11)$$

Unfortunately, the variance of the colored noise $R^{-1}Qg(i, j)$ in $\hat{x}(i, j)$ is large when R is ill conditioned. In such case, the mean-squared error between $x(i, j)$ and $\hat{x}(i, j)$ is large, making $\hat{x}(i, j)$ an unsatisfactory deconvolution estimate. In order to simplify the notation, the equation (11) is rewritten as follows.

$$\hat{x} = x + \gamma \quad (12)$$

In order to attenuate the colored noise γ , in this paper, we focus on simple and fast estimation based scalar shrinkage of individual components in shearlet transform domain. For $t \in \mathbb{R}^+$, define the threshold function $T_t(x)$ to be $x - t \text{sign}(x)$ if $|x| \geq t$. The naïve estimate $\hat{x}(i, j)$ from (11) can be expressed as

$$\hat{x} = \hat{a}_{M_1} \langle \hat{x} + \gamma, y_{j,k,l} \rangle y_{j,k,l} + \hat{a}_{M_2} T_t(\langle \hat{x} + \gamma, y_{j,k,l} \rangle) y_{j,k,l} \quad (13)$$

Where M_1 and M_2 are the indices of approximation coefficients and shearlet coefficients. The shearlet transform is multiresolution and multiscale representation. In this paper, the threshold t is different in different direction l and scale j . And the optimal threshold $t_{j,l}$ is derived by using maximum a posteriori rule. Assuming the color noise density is Gaussian with zero-mean and variance S_n^2 , and $r(x_{j,l})$ is the density of $x_{j,l}$, then the shrinkage threshold

$$t_{j,l} = S_n^2 |x_{j,l}| \quad (14)$$

where $x(x) = -\ln r(x_{j,l})$. In this paper, we assume that the prior distribution of true image shearlet coefficients is a normal inverse Gaussian distribution.

$$f(x_{j,l}) = a \exp\left(-\frac{b}{K_1(x_{j,l})}\right) \frac{1}{K_1(x_{j,l})} \quad (15)$$

where $p(x_{j,l}) = \sqrt{d^2(a^2 - b^2) + bx_{j,l}}$, $q(x_{j,l}) = \sqrt{d^2 + x_{j,l}^2}$, $K_1(x)$ is the modified Bessel function of the second kind with index 1. After substitution of equation (15) in equation (14), we get the adaptive shrinkage threshold $t_{j,l}$.

$$t_{j,l} = s_n^2 |x_{j,l}| = \frac{s_n^2 \sqrt{\frac{a^2}{d^2 + x_{j,l}^2}} K_2 \hat{\otimes} \sqrt{a^2(d^2 + x_{j,l}^2)} \hat{\otimes}}{K_1 \hat{\otimes} \sqrt{a^2(d^2 + x_{j,l}^2)} \hat{\otimes}} \quad (16)$$

We summarize the main steps of shearlet-based inverse half-toning (SIH) algorithm as follows.

1. Operator inversion

Invert the convolution operator R to obtain a noisy estimate $\hat{x}(i, j)$ as in (11).

2. Shearlet-domain thresholding

2.1 Compute the shearlet transform of $\hat{x}(i, j)$ using (7).

2.2 Apply the shearlet shrinkage to shearlet coefficients to obtain estimated coefficients [using (14), (15), and (16)].

2.3 Apply the inverse shearlet transform to the estimated coefficients.

4. EXPERIMENTAL RESULTS

In this section, we illustrate results of the proposed algorithm and compare them with some of other inverse half-toning methods. The tested images are 512x512 Lena, Peppers, Barbara, and Boat half-toned using the Floyd and Jarvis algorithm. In the experimental, we set the gain $K=2.03$.

PSNR is chosen as the objective evaluation criterion. The PSNR values for implementations using different images and different noise levels are list in Table 1. From Table 1, it is seen that the proposed method consistently gives a larger value of PSNR compared to the other methods, which indicating a better preservation of structure in the denoised images, especially to the textured images (such as Barbara).

Table 1. PSNR of different inverse half-toning algorithms

Floyd halftone		
	WInHD [8]	SIH
Lena	31.96	32.59
Barbara	25.71	27.62
Boat	29.19	29.47
Peppers	30.94	31.64
Jarvis halftone		
Lena	32.81	33.60
Barbara	25.33	27.24
Boat	29.78	30.32
Peppers	31.13	31.56

Figure 2 and Figure 3 show the inverse half-toning results of Floyd halftone and Jarvis halftone. From the results we can find that the new proposed method yields the best results. Due to the sparse representation of shearlet transform for curve singularities, the proposed method shows good performance for the edge preserving.

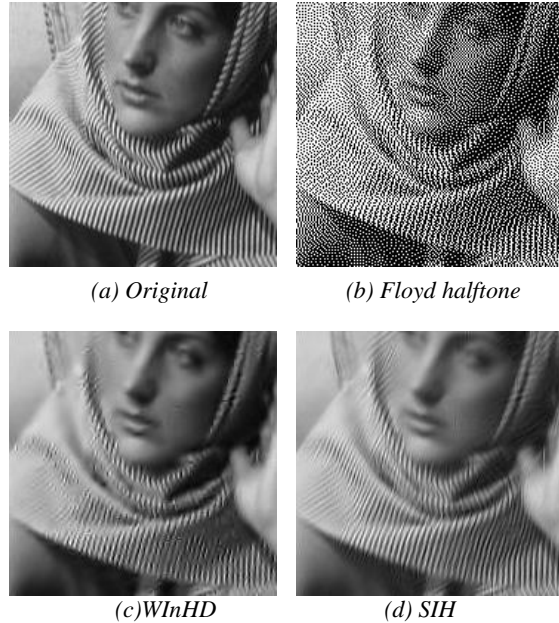


Figure 2. Visual comparison of various methods for Floyd halftone.

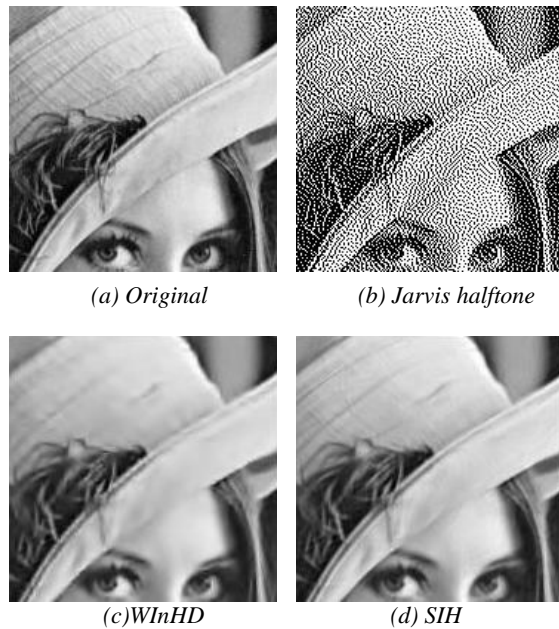


Figure 3. Visual comparison of various methods for Jarvis halftone



5. CONCLUSIONS

In this paper, we proposed a new inverse half-toning algorithm based shearlet. In the new method, the inverse half-toning is posed as a deconvolution problem in the presence of colored noise. The new method performs inverse half-toning by first inverting the model-specified convolution operator and then attenuating the residual colored noise using scalar shearlet shrinkage. And the optimal threshold is estimated by the maximum a posteriori function. Experimental results show that the new method yields state-of-the-art performance. Recently, Liu [16] has proposed inverse half-toning based the Bayesian theorem, which can be employed prior to any signal processing over a half-tone image or the inverse half-toning. In the future, we will focus on Bayesian based inverse half-toning in shearlet domain.

ACKNOWLEDGMENTS

The authors wish to thank the reviewers for their helpful comments and suggestions. This work is supported by the National Natural Science Funds of China under grant 61162022, Natural Science Funds of Jiangxi China under grant 2009GZW0020 and 2010GZW0049, foundation of Jiangxi educational committee under grant GJJ12632, and Key Technology R&D Program of Jiangxi Province China under grant 2011ZBBE50030.

REFERENCES:

- [1] J. Luo, R. de Queiroz, and Z. Fan, "A robust technique for image descreening based on the wavelet transform", *IEEE Trans. Signal Processing*, Vol. 46, No. 4, April, 1998, pp. 1179-1184
- [2] Y. F. Liu, J. M. Guo, J. D. Lee, "Inverse half-toning based the Bayesian theorem", *IEEE Trans. Image Processing*, Vol. 20, No.4, April, 2011, pp. 1077-1084.
- [3] F. L. Zhang, L. Jiao, "An effective image half-toning and inverse half-toning technique based on HVS", *In Processing international Conference on Computational Intelligence and Multimedia Application*, Vol. 1, 2003, pp. 441-445.
- [4] J. Z. Lai, J. Y. Yen, "Inverse error-diffusion using classified vector quantization", *IEEE Trans. Image Processing*, Vol. 7, No.12, December, 1998, pp. 1753-1758.
- [5] Y. H. Huang, K. L. Chung, B. R. Dai, "Improved inverse half-toning using vector and texture-lookup table-based learning approach", *Expert Systems with Applications*, Vol. 38, No. 12, December, 2011, pp. 15573-15581.
- [6] W. B. Huang, A. W. Y. Su, Y. H. Kuo, "Neural network based method for image half-toning and inverse half-toning", *Expert Systems with Applications*, Vol. 34, No. 4, April, 2008, pp. 2491-2501.
- [7] T. D. Kite, B. L. Evans, A. C. Bovik, and T. L. Sculley, "Modeling and quality assessment of half-toning by error diffusion", *IEEE Trans. Image Processing*, Vol. 9, No. 5, May, 2000, pp. 909-922.
- [8] R. Neelamani, R. Nowak, R. Baraniuk, "WinHD: Wavelet-based inverse half-toning via deconvolution", *IEEE Trans. Image Processing*, Vol. 11, No. 5, May, 2002, pp. 919-929.
- [9] Z. Xiong, M. T. Orchard, and K. Ramchandran, "Inverse half-toning using wavelet", *IEEE Trans. Signal Processing*, Vol. 8, No. 10, October, 1999, pp. 1479-1482.
- [10] G. Easley, D. Labate, W. Q. Lim. "Sparse directional image representations using the discrete shearlet transform", *Applied and Computational Harmonic Analysis*, Vol. 25, No. 7, July, 2008, pp.25-46.
- [11] K. Guo, W. Lim, D. Labate, G. Weiss, E. Wilson, "Wavelets with composite dilations and their MRA properties", *Applied and Computational Harmonic Analysis*, Vol. 20, No.2, February, 2006, pp. 231-249.
- [12] K. Guo, D. Labate, and W. Lim, "Edge Analysis and Identification using the Continuous Shearlet Transform," *Applied and Computational Harmonic Analysis*, Vol. 27, No. 1, January, 2009, pp. 24-46.
- [13] V. M. Patel, G. R. Easley, and D. M. Healy, "Shearlet-based deconvolution," *IEEE Trans. Image Process.*, Vol. 18, No. 12, December, 2009, pp. 2673-2685.
- [14] S. Yi, D. Labate, G. R. Easley, and H. Krim, "A Shearlet Approach to Edge Analysis and Detection," *IEEE Trans. Image Process.*, Vol. 18, No. 5, May, 2009, pp. 929-941.
- [15] Q. G. Miao, C. Shi, P. F. Xu, M. Yang, and Y. B. Shi, "A novel algorithm of image fusion using shearlets," *Optics Communications*, Vol. 284, No. 11, November, 2011, pp. 1540-1547.
- [16] Y. F. Liu, J. M. Guo, and J. D. Lee, "Inverse half-toning based on the Bayesian theorem," *IEEE Trans. Image Process.*, Vol. 20, No. 4, April, 2011, pp. 1077-1084.